

Detection and Imaging of He₂ Molecules in Superfluid Helium

W. G. Rellergert, S. B. Cahn, A. Garvan, J. C. Hanson, W. H. Lippincott, J. A. Nikkel, and D. N. McKinsey*

Department of Physics, Yale University, New Haven, Connecticut 06520, USA

(Received 10 September 2007; revised manuscript received 15 November 2007; published 15 January 2008)

We present data that show a cycling transition can be used to detect and image metastable He₂ triplet molecules in superfluid helium. We demonstrate that limitations on the cycling efficiency due to the vibrational structure of the molecule can be mitigated by the use of repumping lasers. Images of the molecules obtained using the method are also shown. This technique gives rise to a new kind of ionizing radiation detector. The use of He₂ triplet molecules as tracer particles in the superfluid promises to be a powerful tool for visualization of both quantum and classical turbulence in liquid helium.

DOI: 10.1103/PhysRevLett.100.025301

PACS numbers: 67.25.D-, 29.40.Gx, 67.25.dk

Ionizing radiation events in liquid helium produce unstable He₂ molecules in both singlet and triplet states [1–4]. The singlet state molecules radiatively decay in a few nanoseconds [5], but the triplet state molecules are metastable because a radiative transition to the ground state of two free atoms requires a strongly forbidden spin flip. The radiative lifetime of the triplet molecules has been calculated to be 18 s in vacuum [6] and measured to be 13 s in liquid helium [7]. Here we present data supporting our previous proposal [8] to detect and image the triplet molecules by driving them through multiple fluorescence-emitting transitions during their lifetime.

The lowest-lying electronic states and two relevant vibrational levels of the triplet molecules are shown in Fig. 1, as well as one cycling transition used to detect them. Two infrared photons can excite a triplet molecule from the ground $a^3\Sigma_u^+$ state to the $d^3\Sigma_u^+$ state. Calculations of the branching ratios indicate that about 10% of the excited molecules will decay to the $c^3\Sigma_g^+$ state, while the remaining 90% will decay to the $b^3\Pi_g$ state, emitting detectable red photons at 640 nm. Molecules in both the $c^3\Sigma_g^+$ and $b^3\Pi_g$ states then decay back to the $a^3\Sigma_u^+$ state, and the process can be repeated. Since the $d^3\Sigma_u^+ \rightarrow b^3\Pi_g$ transition emits a photon that is well separated in wavelength from the excitation photons, scattered laser light can be blocked by appropriate filters. As the entire cycle occurs in roughly 50 ns, it could in principle be repeated enough times to allow for single molecule detection.

The molecular structure complicates matters because molecules in an excited electronic state may decay to excited rotational or vibrational levels of the electronic ground state. If those levels have long relaxation times, and are out of resonance with the excitation lasers, the rate at which a molecule can be cycled is greatly reduced. For He₂ molecules in the liquid, the absorption spectral lines are 120 cm⁻¹ wide [4,9], which is considerably larger than the spacing of the rotational levels (7 cm⁻¹) [10]. The vibrational levels, on the other hand, are separated by about 1500 cm⁻¹ [10], and the vibrational relaxation time is over 100 ms [9]. Therefore, molecules falling to excited vibrational levels of the $a^3\Sigma_u^+$ state are trapped in off-resonant

levels and are lost for subsequent cycles. They can be recovered, however, with the use of repumping lasers. As an example, a molecule that decays to the first vibrational level of the $a^3\Sigma_u^+$ state, $a(1)$, can be driven into the zeroth vibrational level of the $c^3\Sigma_g^+$ state, $c(0)$, with light at 1073 nm (Fig. 1). Our calculations of the Franck-Condon factors imply that a molecule in $c(0)$ will decay back to $a(0)$ around 95% of the time. As there are only two excited vibrational levels below $b(0)$, two repumping lasers are likely all that are needed to ensure that molecules are recovered for high cycling rates in this scheme.

A typical 1 MeV electronic recoil event in liquid helium creates about 32 000 He₂ molecules. About 60% of those molecules are created in the singlet state and 40% are

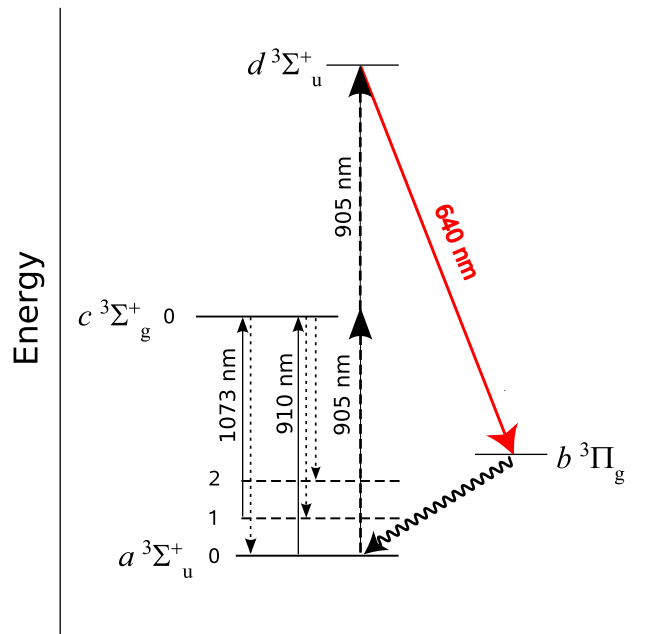


FIG. 1 (color online). Shown schematically are the lowest energy levels of the He₂ triplet molecule in liquid helium. A cycling transition used to detect and image the molecules is indicated, as well as transitions that control the populations of the $a^3\Sigma_u^+$ vibrational levels.

created in the triplet state [11]. For our laser-induced fluorescence studies, we used a $1 \mu\text{Ci } ^{113}\text{Sn}$ beta source immersed in the superfluid ($1.9 \pm 0.1 \text{ K}$) to create the molecules. The 364 keV betas emitted by the ^{113}Sn nuclei deposit most of their energy within 1 cm [11] of the source and create about 2.5×10^8 triplet molecules in steady state. Laser beams illuminate this region, and the resulting fluorescence is recorded with either a photomultiplier tube or a camera as shown in Fig. 2.

Figure 3(a) shows excitation spectra we obtain by scanning a tunable Q -switched pulsed laser [12] in combination with a continuous-wave diode laser. The wavelength of the pulsed laser is scanned from 760 to 1200 nm in steps of 1 nm. The pulse energy is 5 mJ and the repetition rate is 2 Hz. The pulsed laser beam is overlapped with the diode laser beam and both are expanded to a spot size of 1 cm^2 . The solid red curve shows the fluorescence signal as the pulsed laser is scanned with a 60 mW/cm^2 diode laser at 1073 nm. The filters used to block the scattered excitation light allow for the detection of fluorescence in the wavelength range from 515 to 750 nm. Peaks in the fluorescence signal are observed when the pulsed laser wavelength is at either 800 or 905 nm. The wavelength dependence of the fluorescence is measured with a monochromator equipped with short-pass filters that transmit wavelengths less than 875 nm. For both 800 and 905 nm excitation, all observed fluorescence is contained in one peak centered at 640 nm, which is consistent with $d^3\Sigma_u^+ \rightarrow b^3\Pi_g$ emission [Fig. 3(b)]. It should be noted that the wavelength resolution is limited by the slit size of the monochromator. A fit of the average fluorescence signal detected by the photo-

multiplier tube yields $48 \pm 2 \text{ ns}$ for the $d^3\Sigma_u^+$ state lifetime [Fig. 3(c)].

The fluorescence resulting from laser pulses near 800 nm was previously observed by Benderskii *et al.* [13,14]. By calculating potential energy curves for molecules in liquid helium, they determined that the $d^3\Sigma_u^+$ state is shifted up in energy when the molecule is in the liquid. The shift is attributed to the change in size of the bubble formed by the molecule. The two-photon absorption line at 800 nm is therefore thought to drive $a(0) \rightarrow c(1) \rightarrow d(2)$. As the difference in energy between two 905 nm photons and two 800 nm photons is 3000 cm^{-1} , which is roughly twice the expected spacing for the vibrational levels of the $d^3\Sigma_u^+$ state [10], it is likely that the peak at 905 nm is driving $a(0) \rightarrow c(0) \rightarrow d(0)$. As our attempts to produce more fluorescence by using two pulsed lasers at different wavelengths were unsuccessful, a single pulse at 905 nm appears to be the most efficient way to excite the molecules to $d(0)$. Being able to excite the molecules with only one pulsed laser, instead of two as originally proposed [8], is a major simplification. With single wavelength excitation, 2D position information can be obtained by either rastering the laser beam or taking an image with a camera. A second scan (or image) in an orthogonal direction can then yield 3D information.

The dashed blue curve in Fig. 3(a) shows the resulting fluorescence when a 90 mW/cm^2 diode laser at 910 nm is substituted for the diode laser at 1073 nm. Shown schematically in Fig. 1, this laser depletes $a(0)$ by driving

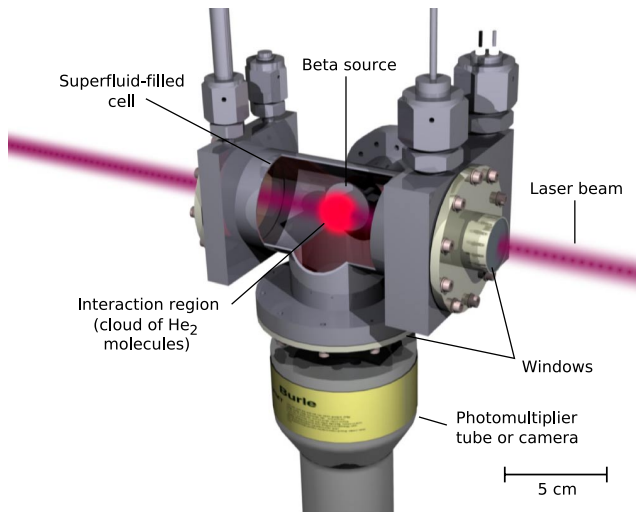


FIG. 2 (color online). Experimental setup. Lasers enter and exit the superfluid-filled cell through 25 mm diameter windows and a light detector views the interaction region through a 25 mm diameter window on the bottom of the cell. The cutaway section in the middle shows the radioactive beta source and the interaction region. The source is deposited on a 25 mm diameter metal disk and is mounted on a flange on the side of the cell. It can also be mounted from the top of the cell.

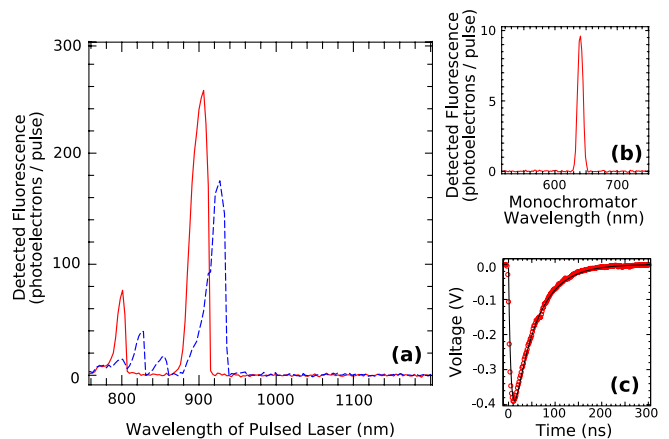


FIG. 3 (color online). Laser-induced fluorescence data. (a) Two excitation spectra obtained by scanning a pulsed laser from 760 to 1200 nm in combination with a diode laser are shown. The solid red line shows the fluorescence signal intensity when a diode laser at 1073 nm is used. The dashed blue line shows the signal when a diode laser at 910 nm is substituted for the 1073 nm diode laser. (b) The wavelength dependence of the fluorescence resulting from laser pulses at 905 nm is measured using a monochromator. All observed fluorescence is centered at 640 nm. (c) The red circles show the average trace from a photomultiplier tube when the pulsed laser is fixed at 905 nm. The black line shows a fit which gives a $48 \pm 2 \text{ ns}$ lifetime for the $d^3\Sigma_u^+$ fluorescence.

molecules into $a(1)$ and $a(2)$, which are long lived. The peaks at 800 and 905 nm are significantly reduced showing that the population of $a(0)$ is indeed lowered, and new peaks in fluorescence are observed at 825, 850, and 925 nm. The suspected excitation scheme for these peaks is $a(1) \rightarrow c(2) \rightarrow d(3)$ for 825 nm, $a(2) \rightarrow c(3) \rightarrow d(4)$ for 850 nm, and $a(1) \rightarrow c(1) \rightarrow d(1)$ for 925 nm.

The ability to repump molecules that fall to $a(1)$ is demonstrated in Fig. 4, which shows the dependence of the fluorescence signal on the pulse number in a sequence of 64 consecutive pulses of 905 nm laser light (2.5 mJ/cm^2). Before the pulse sequence, the laser pulses are blocked with a shutter for 6.4 s to allow the molecules to come to equilibrium. The shutter then opens, and the molecules are excited with a laser pulse every 100 ms for 6.4 s. The shutter then closes, and the process is repeated. Figure 4 shows the average of ten such consecutive pulse sequences both with and without the use of a repumping diode laser. Without a repumping laser, the signal drops to 25% of the initial value by the tenth pulse indicating that molecules are being lost by some mechanism when cycled. With the addition of a diode laser at 1073 nm, however, the signal remains above 85% of the initial value. These data demonstrate that the molecules are indeed being cycled multiple times, that the primary loss mechanism is deexcitations to $a(1)$, and that the molecules in $a(1)$ can be driven back to $a(0)$ by a repumping laser.

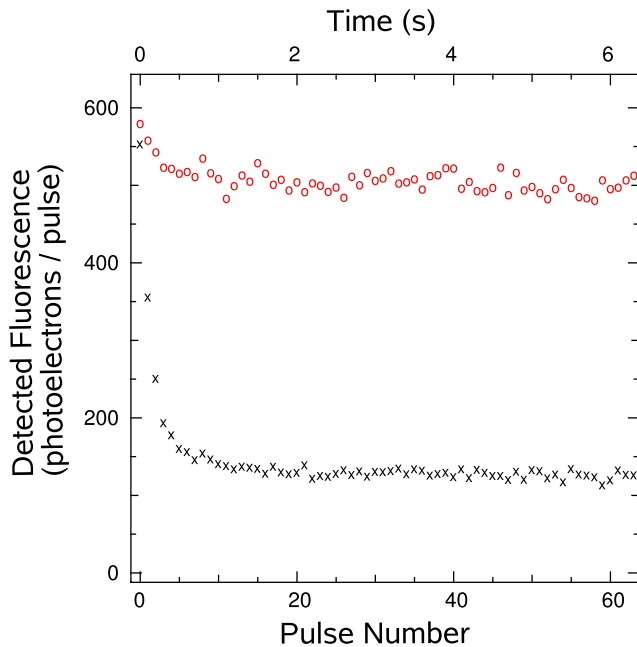


FIG. 4 (color online). These data show the dependence of the fluorescence signal on the pulse number in a sequence of 64 consecutive pulses of 905 nm laser light. Without a repumping laser (black \times 's), the signal drops to 25% of the initial value by the tenth pulse. With the addition of a diode laser at 1073 nm (red circles), however, the signal remains above 85% of the initial value.

The size of the signal in Fig. 4 can be used to obtain a lower bound on the percentage of molecules that are emitting a 640 nm photon. Taking into account the laser beam size and its position, we estimate that it overlaps at most 30% of the molecules produced by the beta source. The solid angle subtended by the photomultiplier tube (0.75%), its quantum efficiency (5%), and the transmission of the various windows and optical filters (30%) indicate that about 1 out of every 10^4 emitted photons are detected. Therefore, detection of more than 500 photoelectrons suggests that for each pulse at least 5% of the molecules in the laser beam are emitting a 640 nm photon.

Images of the molecules are obtained with amplified CCD cameras. A false-color image of the cloud of molecules created by the beta source is shown in Fig. 5(a). The fluorescence is produced by pulsing one laser at 905 nm and a second laser at 925 nm, exciting molecules in both $a(0)$ and $a(1)$. The repetition rate of each laser is 10 Hz, and the pulse energies are 5 mJ. The total exposure time is 5 min. The spatial extent of the cloud agrees with the expected beta particle track length of 1 cm taking into account the 5 mm distance from the laser beam to the source. An image taken with a collimator on the beta source is shown in Fig. 5(b). A single pulsed laser at 905 nm and a 60 mW/cm^2 continuous-wave repumping laser at 1073 nm are used to produce the fluorescence. The repetition rate and pulse energy are again 10 Hz and 5 mJ, respectively, but the exposure time is 2.5 min. As expected, the shape of the cloud is determined by the limited angular spread of the beta particle trajectories.

The technique outlined above gives rise to a new detector technology using liquid helium. In addition to the qualities and applications of such a detector that have already been proposed [8], the method may be useful for a Compton gamma ray imager. If a gamma ray scatters in liquid helium and is subsequently absorbed in a second detector, the locations of those events and total energy deposited can be used to kinematically determine the energy and trajectory of the incoming gamma ray.

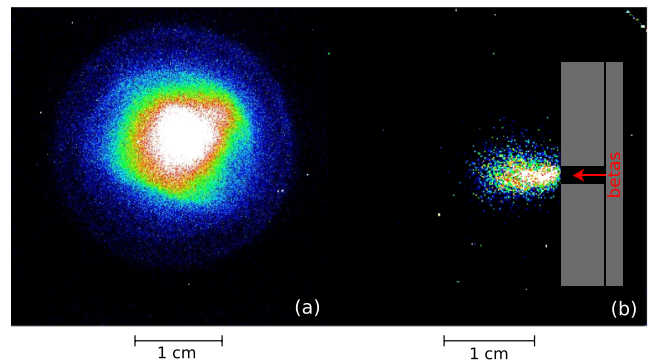


FIG. 5 (color online). Images of the molecules obtained using amplified CCD cameras. In (a) the beta source is facing the camera. In (b) the image is formed by collimating the beta source and imaging it from the side. A sketch of the source and collimator has been added to show its location.

Helium has three characteristics that are desirable for such a detector. First, the low atomic number of helium makes it more likely that a gamma ray will scatter in the liquid rather than be absorbed. Second, the uncertainty in the initial momentum of the electron from which a gamma ray scatters is smaller than it would be for materials with higher atomic numbers, leading to a lower uncertainty in the determination of the initial energy and direction of a scattered gamma ray. Finally, the track of molecules produced by the recoiling Compton electron may be imaged to further reduce the uncertainty in the initial gamma ray direction.

Laser-induced fluorescence of the molecules also provides a new tool for visualization of quantum and classical turbulence in liquid helium [15–17]. Particle image velocimetry has been used to visualize liquid helium flows [18,19], but it appears that the required micron-sized particles are too large to act as passive tracers. A possible reason is their interaction with vortices in the liquid. The He₂ triplet molecules are much smaller (7 Å radius [14]) and should be unaffected by vortices at temperatures above 1 K [20]. Also, the small size of the molecules might allow for resolution of the Kolmogorov length scale. Additionally, at sufficiently low temperatures the molecules will become trapped on vortices [20] as has been observed for ions [21,22] and micron-sized solid hydrogen particles [23]. Stereoscopic imaging of the laser-induced fluorescence of the molecules could then be used to obtain 3D images of vortex lines and their dynamics in the superfluid.

Seeding the flow with the triplet molecules can be done in a relatively easy and unintrusive manner with a radioactive source or an intense, focused laser pulse. By adding a heater in the liquid helium, and monitoring the distribution of the triplet molecules as a function of heater power, one can obtain their diffusion coefficient in the same way that neutron absorption tomography allowed for the determination of the diffusion coefficient of ³He [24]. That information also allows one to obtain velocity fields in liquid helium [25].

In addition, the vibrational levels of the triplet molecule can be used to image and tag a group of molecules in a specific region of the liquid and image their location some time later. For example, after pumping all molecules into $a(0)$, a laser pulse at 800 or 905 nm will result in $d^3\Sigma_u^+ \rightarrow b^3\Pi_g$ fluorescence and also create a population in $a(1)$ which would otherwise not be present. A well collimated laser pulse at one of those wavelengths can therefore be used to image a line of molecules, and, a short while later, a second, expanded laser pulse at 925 nm would show how that line has deformed by imaging those molecules that fell to $a(1)$ after the first excitation. This method is similar to that of a study that used oxygen molecules to measure turbulence in air, and allows one to measure transverse velocity increments which can be used to determine the

single-point probability density of velocity fluctuations [26].

In conclusion, we have detected and imaged He₂ triplet molecules in liquid helium using laser-induced fluorescence. We have demonstrated good control over the vibrational structure of the molecules with the use of continuous-wave diode lasers which allow the molecules to be cycled multiple times over the course of their 13 s lifetime. The cycling rate has so far been limited only by the 10 Hz repetition rate of our lasers.

This work was supported by the Defense Threat Reduction Agency under Grant No. DTRA01-03-D-0009-0011.

*daniel.mckinsey@yale.edu

- [1] H. Fleishman, H. Einbinder, and C.S. Wu, *Rev. Sci. Instrum.* **30**, 1130 (1959).
- [2] C. M. Surko and F. Reif, *Phys. Rev.* **175**, 229 (1968).
- [3] W. S. Dennis *et al.*, *Phys. Rev. Lett.* **23**, 1083 (1969).
- [4] J. C. Hill, O. Heybey, and G. K. Walters, *Phys. Rev. Lett.* **26**, 1213 (1971).
- [5] P. C. Hill, *Phys. Rev. A* **40**, 5006 (1989).
- [6] C. F. Chabalowski *et al.*, *J. Chem. Phys.* **90**, 2504 (1989).
- [7] D. N. McKinsey *et al.*, *Phys. Rev. A* **59**, 200 (1999).
- [8] D. N. McKinsey *et al.*, *Phys. Rev. Lett.* **95**, 111101 (2005).
- [9] V. B. Eltsov, A. Y. Parshin, and I. A. Todoshchenko, *Sov. Phys. JETP* **81**, 909 (1995).
- [10] G. Herzberg, *Molecular Spectra And Molecular Structure Vol. I—Spectra Of Diatomic Molecules* (Krieger, Malabar, FL, 1950).
- [11] J. S. Adams, Ph.D. thesis, Brown University, 2001.
- [12] EKSPLA Model NT342/1.
- [13] A. V. Benderskii *et al.*, *J. Chem. Phys.* **110**, 1542 (1999).
- [14] A. V. Benderskii *et al.*, *J. Chem. Phys.* **117**, 1201 (2002).
- [15] J. J. Niemela and K. R. Sreenivasan, *J. Low Temp. Phys.* **143**, 163 (2006).
- [16] W. F. Vinen, *J. Low Temp. Phys.* **145**, 7 (2006).
- [17] D. Charalambous *et al.*, *J. Low Temp. Phys.* **145**, 107 (2006).
- [18] T. Zhang and S. W. Van Sciver, *J. Low Temp. Phys.* **138**, 865 (2005).
- [19] C. M. White, A. N. Karpetsis, and K. R. Sreenivasan, *J. Fluid Mech.* **452**, 189 (2002).
- [20] W. F. Vinen, in *Low Temperature Physics*, AIP Conf. Proc. No. 850 (AIP, New York, 2006), p. 169.
- [21] E. J. Yarmchuk, M. J. V. Gordon, and R. E. Packard, *Phys. Rev. Lett.* **43**, 214 (1979).
- [22] W. Guo and H. Maris, *J. Low Temp. Phys.* **148**, 199 (2007).
- [23] G. P. Bewley, D. P. Lathrop, and K. R. Sreenivasan, *Nature (London)* **441**, 588 (2006).
- [24] S. K. Lamoreaux *et al.*, *Europhys. Lett.* **58**, 718 (2002).
- [25] M. E. Hayden *et al.*, *Phys. Rev. Lett.* **93**, 105302 (2004).
- [26] A. Noullez *et al.*, *J. Fluid Mech.* **339**, 287 (1997).